A 2700-yr record of Cascadia megathrust and crustal/slab earthquakes from Upper and Lower Squaw Lakes, Oregon

Ann E. Morey (ann@cascadiapaleo.org)
Cascadia Paleo Investigations https://orcid.org/0000-0002-8702-2581
Chris Goldfinger
Oregon State University https://orcid.org/0000-0002-4603-6178

Research Article

Keywords: Cascadia subduction zone, lacustrine paleoseismology, subduction earthquakes

Posted Date: July 17th, 2023

DOI: https://doi.org/10.21203/rs.3.rs-2277419/v2

Abstract

We infer a ~ 2,700-year history of Cascadia megathrust and other earthquakes from two small mountain lakes located 100 km inland of the coast near the California/Oregon border. We use the characteristics of disturbance deposits in the historic portion of the sediment cores from the lower lake to identify a deposit from the 1700 CE Cascadia earthquake (deposit J). This deposit is composed of light-coloured silt (indicating it is enriched in watershed-sourced sediment), without visible mica grains (which would indicate a lake bedrock source), organic grading of the deposit tail, and a basal contact with evidence of rapid loading.

Seven deposits downcore have some of the characteristics of deposit J. An age-depth model suggests that the five deposits most similar to deposit J (including deposit J) are temporal correlatives to the largest margin-wide marine turbidite event deposits from Goldfinger et al., 2012, (T1, T2, T3, T4, T5 and T6), whereas the two deposits with some of the characteristics are potential correlatives of smaller turbidites T5a and T5b. Other thinner deposits are temporal correlatives of T2a and T3a and other smaller deposits of uncertain origin. Lake core physical property data can be correlated to those from other regional lake records and offshore cores. These results suggest that small Cascadia lakes with sufficient sedimentation rates (~ 1–2 cm/decade) with mixed clastic and organic sedimentation may be good recorders of earthquakes, that subduction earthquake deposits are different from those from other types of earthquake deposits and deposits from other types of disturbances, such as floods.

1 Introduction

The hazard posed by Cascadia earthquakes is a function of earthquake size, location, and frequency (Petersen et al., 2020; Priest et al., 2009; Goldfinger et al., 2012; Wang et al., 2013). Evidence of earthquake magnitude comes from estimates of turbidite thickness of offshore seismogenic turbidites (Goldfinger et al., 2012), tsunami size and deposit distribution in coastal marshes in lakes (Kelsey et al., 2005; Witter et al., 2012), and evidence from the spatial pattern and amount of coseismic subsidence (Atwater and Hemphill-Haley 1997; Kelsey et al., 2002, Nelson et al., 2008; Witter et al., 2003; Graehl et al., 2014; Kemp et al., 2018; Nelson et al., 2020).

The most recent research suggests that southern Cascadia has experienced more frequent and variable earthquakes compared to full-margin ruptures (Nelson et al., 2006; Goldfinger et al., 2012; 2013; Morey et al., 2013; Priest et al., 2017; Goldfinger et al., 2017; Milker et al., 2016), however there are uncertainties in the timing and number of events represented in the different records. This uncertainty arises from the location, depositional environment, type of record and dating accuracy and methods used to develop earthquake chronologies. The question of recurrence intervals in southern Cascadia is particularly important because the National Seismic Hazard maps (Petersen et al., 2020) currently rely on the limited data that exists for southern Cascadia, primarily the offshore record of marine seismogenic turbidites (Goldfinger et al., 2012). These records suggest that the southern Cascadia recurrence interval is half that of full margin ruptures (averaged over the Holocene). The tsunami record from Bradley Lake, Oregon

(southern Cascadia; Kelsey et al., 2005; Witter et al., 2012; Priest et al., 2017), with an intermediate recurrence interval of ~390 years, also has fewer tsunamis over a shorter period of time.

Morey et al., 2023 (this volume) suggested that sediment disturbed by earthquakes in Lower Squaw Lake produce deposits that are different from those produced by other types of disturbances, such as floods, and that there are differences among deposits formed in response to subduction earthquakes from those deposited in response to other types of earthquakes. Here we use this information to address the hypothesis that deposit J, attributed to the 1700 CE Cascadia earthquake in Morey et al., 2023 (this volume), was formed in response to shaking from a megathrust earthquake by comparing the frequency and timing of older deposits with similar characteristics to the frequency and timing of published records of pre-1700 Cascadia earthquakes. A result of similar timing and frequency of disturbance deposits in the Squaw Lakes with other types of records of Cascadia megathrust earthquakes would be strong evidence that the sedimentary record from Squaw Lakes, Oregon, record megathrust earthquakes.

2 Methods

2.1 Setting

Upper and Lower Squaw Lakes (42°01'55 N, 123°00'56 W) are located in Klamath-Siskiyou Mountains, ~180 km inland of the trench (Figure 1) at the latitude of the boundary between the Juan de Fuca and Gorda Plates. The lakes were formed when a landslide dammed Squaw and Slickear Creeks near their confluence (Figure 2).

We collected Lower Squaw Lake sediment cores during the summers of 2013, 2014, and 2015. We used a modified Livingstone corer (Wright, 1967), deployed from a custom platform fitted with a stainless-steel pipe attached to two inflatable rafts (2013) or canoes (2014), to collect cores SQB 1, 2, 4,5, 6, 7, and the surface sample (ss) for cores 1 and 2. A Kullenberg piston corer (Kelts et al., 1986) was used to collect cores in 2015. Surface samples from the same locations were collected with a gravity corer. The Kullenberg and gravity coring devices were deployed from a stainless-steel platform attached to a large pontoon-style raft (LacCore; 2015). We acquired single-beam bathymetric data in May 2015 by canoe fitted with a Garmin GPS-enabled “fish finder” and receiver.

We described the sedimentology and deposit characteristics using the following data types: colour (Munsell chart), sediment texture, composition, grading, and contact characteristics as described in Morey et al., 2023 (this volume). Particle-size distribution data (volumetric % by size) were determined by laser diffraction analysis using a Horiba Grain Size Analyzer (LA-920; LacCore) or Beckman Coulter Grain Size Analyzer (LS 13-320; Oregon State University) after organic matter was removed using a 30% hydrogen peroxide solution at 85°C (overnight). Magnetic susceptibility (volumetric; k) was measured using a Bartington MS2E point sensor at 0.5 cm resolution. We acquired combustion data at 0.5–1.0 cm intervals through disturbance deposits and less frequently between these disturbance deposits (cores SQB2 and SQB14 only), resulting in data for the percentage of inorganic content (clastic particles other

than $CaCO_3$), percentage of organic matter (degraded and particulate plant material), and percentage of $CaCO_3$ (calculated from dry weights). We acquired CT (computed tomography) data using a Toshiba Aquillon 64 slice CT unit at the Oregon State University Veterinarian Hospital (at 0.5 mm resolution).

We identified disturbance deposits in cores as abrupt increases in CT density data, as described in Morey et al. (2013). These disturbance deposits were then correlated throughout Lower Squaw Lake using physical property data using modified well-log techniques (Fukuma, 1998; Karlin et al., 2004; Abdeldayem et al., 2004; Hagstrum et al., 2004; Waldmann et al., 2011; Goldfinger et al., 2012; Patton et al., 2015) for cores constrained temporally using ages from detrital macrofossils. Traditional well-log correlations use the physical property data from drilled wells to identify and trace lithologic units. Similarly, this project uses magnetic susceptibility and density data for correlation. This has the benefit of radiocarbon age control data but does not use gamma density or p-wave velocity. These sediment physical property data allow deposits to be correlated based on deposit composition and structure (Amy & Talling, 2006) and is widely used to correlate seismogenic marine turbidites.

We sampled the Lower Squaw Lake cores for radiocarbon after splitting the cores longitudinally. Fragile detrital plant macrofossils sampled from targeted horizons of undisturbed sediment, were cleaned and dried, then analysed by AMS (accelerator mass spectrometer) for radiocarbon. We selected the target horizons for sampling based on a tentative relationship between the dated sequence from Upper Squaw Lake (Colombaroli & Gavin, 2010) and the Lower Squaw Lake stratigraphy. We did not acquire ^{210}Pb and ^{137}Cs data for Lower Squaw Lake cores to get historic sedimentation rate data because the upper portions of the sediment cores contain two thick clastic units (found lake-wide and of varying thickness) with evidence of erosion at the basal contact, which violates the assumptions of these dating methods of continuous sedimentation required to create a sedimentation rate curve. We used the correlation of physical property data, in particular magnetic susceptibility and CT density, between the upper and lower lakes to infer that the younger of these disturbances was deposited in 1964 (as presented in the supplementary data).

An age-depth model for the historic portion of the record was developed from an event-free sequence (e.g., Enkin et al., 2013; Hamilton et al., 2015; Goldfinger et al., 2017) using CT density. The base of each disturbance deposit was determined to be the location where CT density rapidly increases from background sediment and the top of the deposit was determined to be where CT density drops below background levels. Disturbance deposits without evidence of inter-event sedimentation are treated as a single disturbance deposit for the purpose of the age model. Disturbance deposits show significant variability downcore, which complicates the boundary identifications (described in more detail below). A final age-depth model was created using a P_sequence in the Bayesian software OxCal (Bronk-Ramsey, 2017).

2.2 Inferred characteristics for earthquake types

Evidence presented in Morey et al., 2023 (this volume), suggests that there are two types of earthquake-generated disturbance deposits, and that both are different from the deposits of other types of disturbances (i.e., flood deposits) in the historic portion of the record from Lower Squaw Lake. Deposits attributed to earthquakes have organic rich tail deposits, dense silt (sourced from the watershed) at the base and show evidence of loading (detailed below) where the silt lies on the organic-rich sediment below the deposit. Although evidence of loading is not definitive evidence of earthquakes, it is part of the suite of criteria used based on characteristics of deposit J. The types of earthquake-generated disturbance deposits identified and described in Morey et al., 2023 (this volume) are presented below.

Type 1 (Figure 3a). Well-sorted medium silt sourced from the watershed with an organic tail. Example: deposit J, inferred by Morey et al., 2023 (this volume), to result from the ~M9 1700 CE Cascadia earthquake. Deposit J is a thick (~7-15 cm), dense (~1,000 HU at the base), weakly graded, medium to fine-grained silt unit with an organic-rich tail. The base is composed of fine-grained, well-sorted silt (~90% inorganics) that appears “clean” (lacking other components such as broken diatoms and organic matter). The layer of silt is 1.5-4.0 cm thick (depending on location in the lake) and becomes less-well-sorted upward with grading. As grading proceeds upward, the silt becomes more fine-grained, and the organic content gradually increases upward. The particle-size distribution at the base of the deposit is narrower than the rest of the disturbance (as shown in Figures 3a and 3b) and pure (predominantly silt with only trace amounts of diatoms and organic particles). This fine-grained (medium-fine silt) sediment was interpreted to sink into the less-dense sediment below, which we interpret as the result of loading (“LOAD” in Figure 3a). X-ray diffraction (XRD) demonstrates that this silt (sampled from core SQB2A) is composed primarily of sediment sourced from the watershed. Above the deposit tail, background sediment contains a different suite of diatoms compared to prior to the earthquake after the tail deposit suggesting a post-earthquake change in community structure (the types and relative abundance of species living in the water column). It was inferred that the processes triggered by the earthquake removed organisms during settling, altering the types of organisms present in the water column.

Type 2 (Figure 3b). Lake-wide turbidite sourced from lake-margin bedrock. Example: Deposit I from the deposit sequence H/I inferred to result from the ~M7 1873 CE earthquake. The lower portion of the deposit sequence (deposit I) is dark gray (GLEY2 4/5PB) coarse silt dominated by large, visible mica flakes (~90% inorganic). The deposit has a sharp basal contact and is initially reverse, then normally, graded. The reverse-graded portion of the deposit contains a higher percentage of organics (including rootlets) compared to the normally graded portion of the deposit. The base of the deposit is very sharp with evidence of erosion. This deposit is a turbidite deposit which was identified by XRD to be composed of schist (evidence that it is sourced from the lake margin). It is unknown if deposits H and I are the result of the same or separate events.

For this study, we used the distinctive characteristics of deposit J to identify other potential Cascadia earthquake deposits downcore. These characteristics are:

1. Light-coloured (Munsell colour: 2.5Y 4/1, indicating a watershed source), well-sorted silt without visible mica grains.

2. Evidence of loading (projections of silt into the organic sediment below) of the basal silt into the organic-rich sediment below.

3. Presence of a long (typically 2-5 cm but varies with location in the lake) organic-rich tail.

We then used the characteristics of deposit I, inferred to be the result of the 1873 CE Brookings earthquake, to identify other types of earthquakes in the downcore record. This is a lake-wide turbidite composed of dark grey (Munsell colour: GLEY2 4/5 PB, indicating a lake bedrock source) schist containing visible mica flakes and a ~~short~~ (~1 cm) deposit tail.

3 Results

3.1 Identification of earthquake-generated disturbance deposits in Lower Squaw Lake

Disturbance event deposits were identified in the sediment cores used in this study (Table 1) as described in the methods section, then expressed as a correlation diagram (Figure 4). Distinctive beds were correlated using the age data, sedimentology, and physical property data (described further below). Shallow water cores and cores from the northern portion of the lake have less sediment between time equivalent horizons than do the deep water and southern lake cores. The deep-water cores contain thicker disturbance deposits and contain slumps and folds, and occasionally woody debris and portions of soft, partially degraded logs associated with the slumps and folds (labelled on the diagram). A core from the northern site (composite core SQB1/2/ss) was selected to create the chronology to avoid these disturbances in the southern lake cores, avoid an influence from the landslide to the south, and reduce the influence from the second watershed (via Squaw Creek).

Deposits suspected of being triggered by Cascadia earthquakes were identified in the composite core SQB1/2/ss using the characteristics of deposit J as described in the Methods section. Five deposits (deposits K, N, O, R, and X; see Figure 5) were identified as most similar to deposit J in the downcore record. These disturbance deposits are all light-coloured silt layers with few or no visible mica grains, show some evidence of loading into the organic sediment below, and have organic-rich tails. Deposits K and N in the upper portion of the core (Figure 5, bottom left) are most similar to deposit J. These deposits have a well-sorted medium silt that bleeds (fine-grained loading) into the organic sediment below. Deposits O, R and X also have similar characteristics, but are slightly different from, deposit J. For example, deposit O is a thin, light coloured silt with little evidence of loading, deposit R contains evidence of loading as medium silt finger-like projections that are broken off, and deposit X is a large (30 cm long) turbidite showing unusual grading characteristics (including layers of plant macrofossils and benthic

diatoms). None of the labelled deposits has a tail as long as deposit J (the closest is deposit H, which precedes deposit J). These details can be seen in core SQB2 as shown in Figure 5.

Other possible earthquake deposits identified in Chapter 3 are schist layers similar to deposit I. These layers are turbidites that are visible in the cores as dark grey, graded, medium silt layers with visible mica particles. The schist layers sometimes occur before or after the lighter coloured silt layers. Numerous other layers also exist in the cores. These layers have high CT density peaks but are thinner than the other deposits that are suspected to be the result of earthquakes. These disturbances are harder to characterize because they are very thin and therefore difficult to sample. These event deposits do not show evidence of loading and are not composed of light-coloured watershed-sourced silt.

The downcore sequence of disturbance deposits (A-Z) identified in SQB2 (Figure 5) are also shown in the SQB1/2/ss composite core as shown in Figure 6a. Disturbance event deposits identified as most similar to deposit J are identified in orange and disturbances composed predominantly of schist are identified in grey. Background sediment is identified by blue, and other disturbances are shown in black. Event-free depths of horizons are identified in black numbers to the left of the core diagram whereas the red numbers indicate interevent thicknesses (in centimetres).

The relationship between ~~core~~ the lower lake and upper lake cores are shown in Figure 6b. The thickest events in the upper lake core are those identified by Colombaroli et al. (2018) as being outside the distribution of the other silt layers in the record. These layers, identified as disturbances 1-7 in Figure 6b, in the USL 2009 core are correlated to the most prominent disturbances in the lower lake composite core SQB1/2/ss as shown in Figure 6c. This panel also demonstrates how the age data between cores were used to prepare the final age-depth model.

A comparison of Upper and Lower Squaw Lake CT density traces (Figure 6c) demonstrates the strong similarities between records. The thickest event deposits in the Upper Squaw Lake record have a similar timing and frequency as the densest disturbance deposits in the Lower Squaw Lake record, and this relationship is just as strong for the low amplitude variability in the Lower Squaw Lake traces. This similarity allowed for a detailed comparison for age data translation as shown in Figure 6c. The oldest portion of the Upper Squaw Lake record is assumed to be the temporal equivalent of the deposit dated to 1580 +/-20 BP in the Lower Squaw Lake record. The upper and lower lake records can also be seen flattened to one another: SQB1/2/ss was held constant while the USL core data was transformed to line up correlative beds (Figure 6d). The red bars identify the deposit bases that were flattened to the upper lake core.

3.2 Within-lake bed correlation and comparison to Upper Squaw Lake

Disturbance event deposits were initially correlated using physical property data, the age model for core SQB2, and individual ages from other cores. This was straightforward for cores where the same horizon

was dated in multiple cores, but this was only the case for the horizon ~1200 BP in cores SQB2, SQB14 and SQB5. The majority of the 14C ages were from core SQB2 (7 samples), one at the base of SQ5, 3 samples from SQB14 and one sample from SQB10. The basal age from SQB14 and the age from SQB10 were too old to be used to date the horizon they were sampled from based on correlation of the cores using the physical property data.

The physical property data reflect the characteristics and amount of clastics in the cores. Whereas CT density and magnetic susceptibility in turbidite deposits from marine sediment cores are primary a function of mineralogy and grain size (Goldfinger et al., 2012), these physical properties reflect mineralogy and % organic matter in the Lower Squaw Lake cores. For example, deposits that have a higher concentration of watershed-sourced sediment compared to lake margin schist have higher CT density and magnetic susceptibility values, a function of the characteristics of the mineralogy. Likewise, the amount of organic matter in the deposit influences the magnetic susceptibility and CT density because there is a smaller percentage of clastic particles. This is also evident for the tail of deposit J (Figure 3a) where CT density is a sensitive indicator of the inorganic content (see Figure 12 in Morey et al., 2023 (this volume), for a comparison between CT density and loss on ignition % inorganic data).

Physical property data, particularly the sub mm-scale CT density, can be used to match patterns in lithology downcore. Some of the cores contain a large amount of gas (methane) as pockets within the cores, which causes HU values to drop suddenly. This is not a problem for the northern composite core SQBss/1/2. Although the noisy data can complicate matching the downcore patterns, the patterns dominate the CT density variability, and it is possible to correlate beds and even low-amplitude signals throughout the lake.

Colombaroli et al., 2018, identify seven thick silt deposits that are outside the frequency magnitude (power law) relationship of silt events in the Upper Squaw Lake core (Colombaroli et al., 2010; 2018). Although these thick units appear homogenous because of similar particle size (medium silt) throughout the deposit (until the very top, where it becomes a silty-clay cap), there are compositional differences that result in a slight increase in density from the base of the deposit to the top (Figure 9). The very thin (mm-scale) silty-clay cap at the top would be expected if most of the fine sediment suspended in the water column is transferred into Lower Squaw Lake via Squaw Creek. The Upper Squaw Lake deposits do not have an organic tail but are followed by a sequence of progressively thinner silt layers before returning to normal sedimentation. These seven silt deposits can be identified as correlative units in the Lower Squaw Lake record (numbered events in Figure 6).

3.3 Lower Squaw Lake age-depth model

The radiocarbon determinations used in the age-depth model are listed in Table 2. Radiocarbon samples in bold were used in the age-depth model, and those in grey were not (determined based on the relationship between sample locations cores and relative ages). The radiocarbon datums were translated from Upper Squaw Lake onto composite core SQBss/1/2 after the stratigraphic sequences were aligned

(Figure 6c,d). The age and depth data were then used to create the Lower Squaw Lake age-depth model shown in Figure 7 (using OxCal as described in the methods section using the assumptions presented in Morey et al., 2023, this volume).

3.4 Lower Squaw Lake Cascadia disturbance event chronology

Based on the age-depth model for the Lower Squaw Lake composite core SQBss/1/2, the ages for the deposits identified as likely the result of a major disturbance event are shown in Table 3. Disturbance event deposits DE-S and DE-W are italicized because the deposits have some, but not all, of the characteristics of deposit J. Both deposits show evidence of loading, but do not have a distinctive and discrete light coloured silt layer like the other deposits. Deposits DE-S through DE-X have large age ranges because of the limited age control data at those depths in the cores.

4 Discussion

4.1 Origin of the disturbance event beds

The timing and frequency of disturbance deposits composed of watershed sourced silt (shown in Figure 6 and listed in Table 3) are similar to the timing and frequency of Cascadia earthquakes. The thickest of these beds correlate to the thickest beds from the Upper Squaw Lake record. If bed thickness is a shaking duration proxy, then they might be expected to correlate.

Sediment and water are required to create earthquake-triggered disturbance deposits in lakes. Water transports sediment to the lake and the sediment is deposited, loading the lake margins. Whereas water supply is a function of climate, vegetation, substrate and watershed size and characteristics, sediment supply can fluctuate as a result of changes in landcover (from changes in climate or as a result of wildfires), or as a result of human activities such as logging and road building. Likewise, with a sufficient supply of sediment and water, sediment can also be transported to the lake to create flood-induced disturbances.

Physical property peaks in lake sediment cores can be the result of a variety of events. These include 1) aseismic events such as post-fire erosion, storm remobilization of sediment, land-use changes and flooding, 2) seismic events which trigger landslides and submarine lake floor sediments, 3) mixed seismic and aseismic events, such as the destabilization and subsequent transport of destabilized hillslope sediment into the lake, 4) concentrations of authigenic minerals such as magnetite, 5) shaking from nearby volcanic activity, and 6) layers of volcanic tephra. This study seeks to differentiate between plate boundary earthquake, non-plate boundary earthquakes, and aseismic disturbance deposits triggered in-lake disturbances by comparing the record of disturbances from Squaw Lakes to published records of

Cascadia megathrust earthquakes. First, however, we determine if the beds are internally (within-lake) or externally (watershed) sourced.

4.1.1 Post-fire and flood-related erosional events

Lakes throughout Cascadia have been used extensively to reconstruct fire histories and post-fire erosion, where minerogenic layers and charcoal abundance data are frequently used to infer increased erosion after large wildfires (e.g., Millspaugh and Whitlock, 1995; Colombaroli and Gavin, 2010). Although charcoal analysis has been successfully used as a proxy for post-fire erosional events, Long et al. (1998) show that peaks in charcoal accumulation do not always correlate with magnetic susceptibility at Little Lake, Oregon. Similarly, charcoal peaks at Bolan Lake, Oregon, and Sanger Lake, California, (between the coast and Squaw Lakes at a similar latitude) are not always associated with (or immediately precede) magnetic susceptibility peaks (C. Briles, pers. comm., 2010).

Although wildfires are common in Cascadia and charcoal analysis at nearby Upper Squaw Lake suggests that wildfires do influence erosion in this region (Colombaroli and Gavin, 2010), subsequent analysis of the pseudo-annual silt layers observed in the CT data has suggested that the seven largest disturbance events in the record (pre-logging era) are the result of a different process at Upper Squaw Lake other than erosion, possibly earthquakes (Colombaroli et al., 2018). The study demonstrates that although the rate of silt deposition (mm/year) displays a power law distribution, there are seven largest silt layers that are thicker than expected, suggesting a different process controls the silt accumulation during those times.

Runoff-initiated post-fire subaerial debris flows have been observed to be a significant erosional process in the Western Cascades, Oregon (Wall et al., 2020). These debris flows could create hyperpycnal flows resulting in thick debris flow deposits (such as turbidites and hyperpycnites) and must be considered as a possible origin for the seven largest deposits in the Upper Squaw Lake record. This is considered unlikely, however, because the correlative units in the Lower Squaw Lake record do not show evidence of basal erosion (coarse basal sediment and entrained organic matter) as would be expected for a debris flow deposit. For example, a comparison of the basal layer of deposit B (assumed to be a debris flow turbidite) and deposit J (attributed to the 1700 CE Cascadia earthquake) are different in the following ways. Whereas both basal silt layers have roughly the same amount of clastic material (~90% by weight) their compositions are completely different. The base of deposit B is composed of poorly sorted coarse-grained silt and contains degraded and particulate organic matter including rootlets which affects the magnetic susceptibility of the lower half of the deposit. In contrast, the base of deposit J is composed of very well-sorted medium-grained silt and contains very little degraded organics, few visible particulate organics, and magnetic susceptibility is high throughout the silt. Although the grain-size of the deposits similar to deposit J increase in grain-size (to coarse silt) downcore, the other characteristics of the deposit are very similar (high magnetic susceptibility, less degraded and particulate organics, and narrow particle size range).

Both floods and post-fire erosion, however, may be a source for the smaller deposits in the Lower Squaw Lake record other than those that are correlated to the seven thickest deposits in the Upper Squaw Lake record. Flood disturbances have been identified in the Lower Squaw Lake record (presented and discussed in chapter 3) as deposits with slight increasing, then decreasing, grain size and % clastics with a physical property profile that is somewhat rounded in appearance, typical of the waxing and waning of storm events (Mulder, 2001). This is also supported by data from St-Onge et al. (2004) who analysed a sedimentary sequence from Saguenay Fjord, Québec, that was produced from a known historic earthquake followed by a flood (landslide dam breach). The analysis showed that the hyperpycnite deposit resulting from the flood has reverse, then normal, grading whereas the earthquake-triggered turbidite deposit has normal grading.

At Upper Squaw Lake, silt accumulation was strongly correlated with precipitation during the logging era (1930-present), however prior to that time the occurrence of the thicker silt layers (other than the seven thickest) was related to fire (determined because they were preceded by high charcoal concentrations). This suggests that at this location (Squaw Lakes) flood deposits are not the thickest silt units and where present in the lower lake, even the largest historic flood layers appear to have a rounded appearance in their physical property data (see for example, deposit G and the deposit suspected to be the result of the extreme flood from the 1861-62 atmospheric river event flood just below deposits H and I).

4.1.2 Earthquakes

Morey et al., 2023 (this volume), suggests that plate boundary, intraplate and/or crustal earthquakes influence the record at Squaw Lakes. To evaluate this, we first use what is known from the historic portion of the record to suggest interpretations based on the sedimentology, then we compare the temporal relationship between the Lower Squaw Lake record and nearby paleoseismic records of Cascadia earthquakes.

4.2 Deposits similar to Deposit J

4.2.1 Temporal relationship to nearby paleoseismic events (marine and coastal)

Figure 6a identified the 26 disturbance deposits, DE's A-Z, that have large excursions in magnetic susceptibility in the downcore record from Lower Squaw Lake. Nine of these disturbance event deposits (Table 3; including deposit J and deposit H) have some of the characteristics of deposit J, which was suggested in Morey et al., 2023 (this volume), to have formed in response to ground motions from the 1700 CE Cascadia earthquake. The other disturbance deposits identified in the downcore record are also of higher density and magnetic susceptibility compared to background sediment, but do not have a distinctive watershed sourced composition or some of the other characteristics of deposit J.

Table 4 identifies the beds from Lower Squaw Lake and possible correlatives from marine and coastal paleoseismic data– the T numbers in bold are the thickest beds at Rogue Apron site which are also those deposits that correlate to beds at Hydrate Ridge West (Figure 8; both of which are marine turbidite sites from Goldfinger et al., 2012). This suggests that the disturbances with watershed-sourced silt, organic tails, and evidence of loading from the Lower Squaw Lake record are most likely the result of significant plate boundary earthquakes (identified in Goldfinger et al., 2012, and summarized in Walton & Staisch et al., 2021). These characteristics are consistent with, but not exclusive to, earthquake triggered events.

Table 4 indicates that there is an excellent temporal match between the four coastal, lake and marine paleoseismic sites for the margin-wide events T1, T2, T3, T4, and T5 (using the marine turbidite bed notation). T1/DE-J, T3/DE-N, and T4/DE-O correlatives have radiocarbon determinations which are within a few decades, whereas there is poorer agreement between T2/DE-K and T5/DE-R medians and ranges even though the ranges overlap significantly (some ranges are simply larger than others). Although DE-X is suspected to correlate to T6 (based on a comparison of physical property data between lake and marine cores), the age range for DE-X is significantly larger (460 yrs for DE-X compared to a few hundred years for Rogue and Hydrate Ridge sites) making this linkage less certain. A distinctive 1000 yr gap occurs in the record of Cascadia earthquakes between T5 and T6 in all records (Atwater 2004; Kelsey et al., 2005; Goldfinger et al., 2012; and Witter et al., 2012). This can be seen in the Lower Squaw Lake record as well. A graphical representation of the relationships between these age distributions can be seen in Figure 8.

4.2.2 Correlation of physical property data between Lower Squaw Lake and the marine paleoseismic record

The Lower Squaw Lake record was correlated to marine sites Rogue Apron and Hydrate Ridge Basin West (Goldfinger et al., 2012; see Figure 1 for core locations) using physical property and radiocarbon data. The relationships between cores are shown in the bed-flattened correlation diagram (Figure 9). This method of correlation appears to work even though the physical property data for the marine cores typically reflects the amount of magnetic minerals and grain size of horizons downcore, whereas the physical property data is also influenced by the percentage of organic matter (which can be part of the graded sequences) in the lake core.

4.3 Smaller disturbance event beds

There are smaller deposits in the Squaw Lake sequence that were not identified as potential Cascadia megathrust earthquake deposits because they do not have the characteristics of deposit J described in Morey et al., 2023 (this volume). Some of these may correlate to the large number of smaller deposits in the marine record. Deposit L is one example. This deposit is dark grey turbidite with visible mica flakes, and therefore is more similar to the wall failure deposit E and seismoturbidite deposit I described in Chapter 3. This deposit has a correlative unit in the Upper Squaw Lake record (dated to 550-670 BP, two-

sigma range, Figure 6) and is contemporaneous with marine event T2a. The different composition (schist) and characteristics (it is a turbidite with a short tail) of this deposit in the lake core suggests that it was not a Cascadia earthquake that triggered this deposit. It also does not match the timing of anything on the northern San Andreas fault (nor do T2b, T3a, or T4a; see Goldfinger et al., 2019, 2020). For these smaller events our uncertainty is higher because we can't use size of the event (because frequency is a function of distance), and there is more uncertainty in timing. These events, then, are harder to interpret. Lakes as well are not perfect recorders and therefore we cannot simply say an earthquake occurred or didn't occur simply based on the physical property data. Based on the available information, however, our preferred interpretation is that the thickest of these schist layers are the result of separate events and not complex deposits in response to shaking from an earthquake because they occur in various combinations (as a single deposit, and before and after the initiation of a Cascadia-like deposit) relative to Cascadia earthquakes. Without further information, because T2a, T2b, and T4a are not San Andreas fault earthquakes and they are present in the Upper and Lower Squaw Lakes records as well as at Rogue and other southern Cascadia sites, it is suggested that they may be the result of southern ruptures of the Cascadia fault.

Other sources of seismicity may also influence these records: earthquakes on crustal faults (such as the San Andreas fault or other unidentified regional faults), the Gorda Plate, nearby transform faults, and intraplate earthquakes. There have been suggestions that both the M7.9 1906 CE San Andreas earthquake and the ~M7.0 1873 CE Brookings intraplate earthquake are found in both the marine and lake records (Morey et al., 2023 (this volume), and Goldfinger, 2019; 2020). For example, other regional lakes, such as Bolan and Sanger Lakes, both potentially contain evidence of T2 and T2a, although the resolution of the Bolan Lake record has less-distinct deposits compared to Sanger Lake (see Figure 10). This work is ongoing and beyond the scope of the work presented in this article.

4.4 Data integration

The correlation between the Lower Squaw Lake disturbance record and Rogue Canyon and Hydrate Ridge marine sediment cores (Figure 9) suggests that all the full-margin ruptures (T1-T6), including T2 (using the marine turbidite T numbers from Goldfinger et al., 2012), younger than 2700 BP disturb sediments in Lower Squaw Lake. T2 is unusual because it is not found in any of the coastal southern Cascadia paleoseismic sites (Coquille River, Bradley Lake, and Sixes River; Kelsey et al., 2005; Witter et al., 2012) but is found in the marine turbidite record of Goldfinger et al. (2012; 2013). These southern coastal sites record tsunamis, and to have created a deposit at the site the tsunami must have been large enough to have entered the lake or estuary. Megathrust earthquakes that produced turbidite deposits T1, T3, T4, T5 and T6 caused large tsunamis at Bradley Lake (Figure 8). It is possible that T2, a smaller turbidite, may have been triggered by a smaller earthquake which produced a smaller tsunami that did not overcome the threshold to leave a deposit at Bradley Lake or other coastal sites.

Although T3a, a southern Cascadia event, was not identified as an individual disturbance event deposit in the Lower Squaw Lake record, there is a disturbance event with a smaller magnetic susceptibility and CT density signature in the core. This suggests that even these smaller disturbance events in the Lower Squaw Lake record may be the result of Cascadia earthquakes.

The timing of T5 and T6 are similar to the timing of the formation of Lower Squaw Lake (2470-2700 BP; ~T6) and Upper Squaw Lake (1420-1530 BP; ~T5). Did shaking from a megathrust earthquake cause the landslide to fail, creating the lakes or are failures of the landslide the result of nearby crustal faults? High-frequency ground motion from a nearby intraslab earthquake is suspected in Morey et al., 2023 (this volume) to be the cause of the landslide dam failure in 1873 CE, suggesting that local earthquakes can disturb the landslide, however it is also possible that the landslide is unrelated to earthquakes. This is important because there have been several studies that have attempted to link landslides in the Coast Range and elsewhere to Cascadia earthquakes without success (see, for example, Struble et al., 2020 and LaHusen et al., 2020).

The correlation between physical property data between the Upper and Lower Squaw Lakes records and the Rogue Apron and Hydrate Ridge West marine seismoturbidite records (Figure 9) suggest that these sites are being influenced by the same events. Given this large-scale correlation over multiple depositional environments it would be expected that nearby lakes would also contain similar types of event deposits that are easy to correlate, however this is not so (Figure 10). There are several reasons for this. First, the lakes are very different from one another. Both Bolan and Taylor lakes are spring fed, with little clastic supply, resulting in disturbance events that are difficult to see without very high-resolution data and a careful examination of the sedimentology of the cores. Sanger Lake is slightly different in that it is a cirque lake with a large glacial rock fall upstream of the lake. Strong ground motion could cause settling of the large boulders and cobbles, resulting in the thick lake-wide clay layers interpreted to be the result of the earthquakes that caused the marine deposits T1 and possibly T4 (Figure 10). Why these earthquakes would produce these thick layers (and not the other large earthquakes), is unknown. Again, high resolution data, in particular CT data, colour imagery and high-resolution point magnetic susceptibility data, in conjunction with careful examination of the stratigraphic sequences is required to understand the sedimentary record from this site. Furthermore, it is imperative that the sediment cores be carefully evaluated prior to sampling for radiocarbon to avoid sampling from organic disturbance layers that are frequently formed in response to shaking in lakes dominated by organic sedimentation.

It is also possible that some lake types are more conducive to preserving evidence of earthquakes than others. Based on this study the following characteristics of lakes are suggested as optimal sites for paleoseismic studies in Cascadia:

1. Small lakes (< 1 km^2); landslide dammed lakes.

2. High sedimentation rates (~1-2 cm/decade); mixed (roughly 50% each) clastic and organic sedimentation.

3. The presence of a delta as a source of fine material for liquefaction.

4. Water depth greater than ~7 meters to prevent an influence from bioturbation.

5 Summary and Conclusions

Seven of the 26 disturbance event deposits identified in this chapter have the characteristics of deposit J, which has been attributed to the 1700 CE Cascadia megathrust earthquake. These disturbances correlate to the thickest disturbances in the Upper Squaw Lake record, and to full margin megathrust events onshore coastal and offshore marine turbidite records over the past 2700 years: T1, T2, T3, T4, T5 and possibly T6 (as interpreted by Goldfinger et al., 2012; other interpretations of the onshore and offshore data exist). There are smaller events in the Lower Squaw Lake record as well. T2 and T2a marine equivalents are missing in the tsunami record from Bradley Lake, however both have temporal equivalents present in Lower Squaw Lake. Most of these smaller events cannot be attributed to specific events, however there is the potential to sort this out in the future with further analysis and additional radiocarbon ages. For example, although T3a was not identified as a significant disturbance in the Lower Squaw Lake record, there is a smaller disturbance below T3 that could be dated to determine if it is contemporaneous with T3a in the offshore record.

Some of the smaller events are schist layers which appear to be independent responses to a single event not part of a complex as interpreted in Morey et al., (this volume). Table 4 shows that the Lower Squaw Lake record has the temporal equivalents of T2a, T4a, T5a, T5b and T5c. The only event missing in this time range is T3a. Of these, T2a, T4a and T5b are interpreted as possible crustal events, while T5a and T5c equivalents are more similar to plate boundary earthquakes. So, it seems possible that there are mixed sources for these smaller southern events, but it is not possible to tease them apart without more information.

The relationship between regional lakes needs further investigation into the sedimentology and fine-scale details of the stratigraphy to interpret, however there is evidence that regional cores also contain evidence of Cascadia earthquakes. The signal is not as strong, but this may be a result of the lack of high-resolution data, especially CT data, for these cores. The strength of the signal in these cores (Bolan and Sanger lakes) may be a result of the lack of clastic supply because they are primarily spring fed lakes. This suggests that landslide dammed lakes or those that are stream fed may be better sources because they load the lake margin with sediment and create deltas, both of which are conducive to producing disturbance event deposits in lakes.

Declarations

Acknowledgements

This research was partially supported by the National Earthquake Hazards Reduction Program of the U.S. Geological Survey (through a grant to Andrew Meigs and Simon Engelhart, USGS Grant G17AP00028).

The USGS Earthquake Hazards Program through Alan R. Nelson (USGS, Golden) partially supported the collection of some Livingstone cores and CT scans of Livingstone and Kullenberg cores. Geological Society of America awards provided additional funding: a graduate student research grant and the Kerry Kelts Limnogeology Award. Coring in 2015 would not have been possible without contributions from Joseph Stoner, Roy Haggerty, and a donation from Ruth Morey.

The US Forest Service granted permission for this study (special thanks go to Starr Ranger Station employees and the regional office in Grants Pass, OR). We are extremely grateful for the assistance and knowledge provided by Ranger John McKelligott, and for field assistance by Mark Anthony (USFS employee who participated in coring in 2015). Bert Harr generously allowed access to his Slickear Creek property during this investigation and contributed significantly to this project through his vast knowledge of local extreme events and local and regional history since 1900. Peter Jones provided personal historic accounts of the more recent historic floods.

This project could not have happened without the generous assistance from numerous volunteers. Dan Gavin (UO) and Alan R. Nelson (USGS-Golden) provided coring equipment, expertise, and guidance during this project. Katie Alexander (Western Washington University) spent a few days canoeing in the cold to acquire bathymetric data. Maureen Walczak (OSU) generously analyzed my first radiocarbon samples and provided guidance on how to use the radiocarbon production curve to select samples. Jamie Howarth (then at GNS, NZ) provided useful coring information and guidance, including sharing his approach to dating an earthquake event in lake sediments from about the same time as the 1700 CE Cascadia earthquake. Other volunteer field assistants included Randy Keller, Brendan Reilly, Katie Alexander, and many others. Christy Briles (Colorado University, Denver) helped train me in the fine art of lake coring during a fateful summer week in 2010.

LacCore and the University of Minnesota, provided Kullenberg coring equipment and expertise. Mark Shapley, my LacCore contact, provided guidance, knowledge, and enthusiastic discussions about data. Thanks also go to the OSU core repository (especially Maziet Cheseby) for housing cores and providing the tools to process them. Carol Chin aided core processing of the Kullenberg cores, for which I am extremely grateful.

References

Abdeldayem, A. L., Ikehara, K., & Yamazaki, T.: Flow path of the 1993 Hokkaido-Nansei-oki earthquake seismic turbidite, southern margin of the Japan sea north basin, inferred from anisotropy of magnetic susceptibility. Geophysical Journal International, 157(1), 15–24. https://doi.org/10.1111/j.1365-246X.2004.02210.x, 2004.

Amy, L.A., and Talling, P.J.: Anatomy of turbidites and linked debrites based on long distance (120 × 30 km) bed correlation, Marnoso Arenacea Formation, Northern Apennines, Italy: Sedimentology, v. 53, p. 161–212, doi: 10 .1111 /j .1365 -3091 .2005 .00756 .x, 2006.

Atwater, B. F., & Hemphill-Haley, E.: Recurrence intervals for great earthquakes of the past 3,500 years at northeastern Willapa Bay, Washington (No. 1576). US Government Printing Office, 1997.

Atwater, B. F., Tuttle, M. P., Schweig, E. S., Rubin, C. M., Yamaguchi, D. K., and Hemphill-Haley, E.: Earthquake recurrence inferred from paleoseismology, in Gillespie, A. R., Porter, S. C., and Atwater, B. F., eds., The Quaternary period in the United States, Volume 1, Elsevier p. 331-350, 2004.

Bronk Ramsey, C.: OxCal Program (Version 4.3.2) [Computer software]. Oxford University Research Lab for Archaeology. https://c14.arch.ox.ac.uk/oxcal.html, 2017.

Colombaroli, D., & Gavin, D. G.: Highly episodic fire and erosion regime over the past 2,000 y in the Siskiyou Mountains, Oregon. Proceedings of the National Academy of Sciences, 107(44), 18909–18914. https://doi.org/10.1073/pnas.1007692107, 2010.

Colombaroli, D., Gavin, D. G., Morey, A. E., & Thorndycraft, V. R.:. High resolution lake sediment record reveals self-organized criticality in erosion processes regulated by internal feedbacks. Earth Surface Processes and Landforms, 43(10), 2181–2192. https://doi.org/10.1002/esp.4383, 2018.

Enkin, R. J., Dallimore, A., Baker, J., Southon, J. R., & Ivanochko, T.: A new high-resolution radiocarbon Bayesian age model of the Holocene and Late Pleistocene from core MD02-2494 and others, Effingham Inlet, British Columbia, Canada; with an application to the paleoseismic event chronology of the Cascadia Subduction Zone. Canadian Journal of Earth Sciences, 50(7), 746–760. https://doi.org/10.1139/cjes-2012-0150, 2013.

Fukuma, K.: Origin and applications of whole-core magnetic susceptibility of sediments and volcanic rocks from Leg152. In Proceedings of the Ocean Drilling Program (Vol. 152, pp. 271-280), 1998.

Goldfinger, C., Galer, S., Beeson, J., Hamilton, T., Black, B., Romsos, C., Patton, J., Nelson, C. H., Hausmann, R., & Morey, A.: The importance of site selection, sediment supply, and hydrodynamics: A case study of submarine paleoseismology on the northern Cascadia margin, Washington USA. Marine Geology, 384, 4–16, 17, 25–46. https://doi.org/10.1016/j.margeo.2016.06.008, 2017.

Goldfinger, C., & Gutierrez, J.: Possible stratigraphic evidence of stress triggering of the northern San Andreas fault following southern Cascadia earthquakes. Proceedings of the American Geophysical Union (pp. OS54A-03). San Francisco, CA, US, 2019.

Goldfinger, C., Black, B., Patton, J.R., Beeson, J., Morey, A.E., Nelson, C.H.: Calibrating the Smallest Southern Cascadia Earthquakes with Historic Turbidite Stratigraphy, American Geophysical Union Fall Meeting, Abstract NH004-04.

Goldfinger, C., Morey, A. E., Black, B., Beeson, J., Nelson, C. H., & Patton, J.: Spatially limited mud turbidites on the Cascadia margin: Segmented earthquake ruptures? Natural Hazards and Earth System Sciences, 13(8), 2109–2146. https://doi.org/10.5194/nhess-13-2109-2013, 2020.

Goldfinger, C., Nelson, C. H., Morey, A. E., Johnson, J. E., Patton, J. R., Karabanov, E. B., Gutierrez-Pastor, J., Eriksson, A. T., Gràcia, E., Dunhill, G., Enkin, R. J., Dallimore, A., & Vallier, T.: Turbidite event history: Methods and implications for Holocene paleoseismicity of the Cascadia subduction zone (US Geological Survey Professional Paper 1661-F). https://doi.org/10.3133/pp1661F, 2012.

Graehl, N. A., Kelsey, H. M., Witter, R. C., Hemphill-Haley, E., & Engelhart, S. E.: Stratigraphic and microfossil evidence for a 4500-year history of Cascadia subduction zone earthquakes and tsunamis at Yaquina River estuary, Oregon, USA. GSA Bulletin, 127(1-2), 211-226, 2015.

Hagstrum, J. T., Atwater, B. F., & Sherrod, B. L.: Paleomagnetic correlation of late Holocene earthquakes among estuaries in Washington and Oregon. Geochemistry, Geophysics, Geosystems, 5(10), 2004.

Hamilton, T. S., Enkin, R. J., Riedel, M., Rogers, G. C., Pohlman, J. W., & Benway, H. M.: Slipstream: an early Holocene slump and turbidite record from the frontal ridge of the Cascadia accretionary wedge off western Canada and paleoseismic implications. Canadian Journal of Earth Sciences, 52(6), 405-430, 2015.

Karlin, R. E., Holmes, M., Abella, S. E. B., Sylwester, R.: Holocene landslides and a 3500-year record of Pacific Northwest earthquakes from sediments in Lake Washington. Geological Society of America Bulletin, 116(1), 94–108. https://doi.org/10.1130/B25158.1, 2004.

Kelsey, H. M., Nelson, A. R., Hemphill-Haley, E., & Witter, R. C.: Tsunami history of an Oregon coastal lake reveals a 4600 yr record of great earthquakes on the Cascadia subduction zone: Geological Society of America Bulletin, 117(7–8), 1009–1032, https://doi.org/10.1130/B25452.1, 2005.

Kelsey, H. M., Witter, R. C., & Hemphill-Haley, E.: Plate-boundary earthquakes and tsunamis of the past 5500 yr, Sixes River estuary, southern Oregon. Geological Society of America Bulletin, 114(3), 298–314, https://doi.org/10.1130/0016-7606(2002)114<0298:PBEATO>2.0.CO;2, 2002.

Kelts, K., Briegel, U., Ghilardi, K., & Hsu, K.: The limnogeology-ETH coring system. Swiss Journal of Hydrology, 48(1), 104–115. https://doi.org/10.1007/BF02544119, 1986.

Kemp, A. C., Cahill, N., Engelhart, S. E., Hawkes, A. D., & Wang, K.: Revising Estimates of Spatially Variable Subsidence during the AD 1700 Cascadia Earthquake Using a Bayesian Foraminiferal Transfer Function. Bulletin of the Seismological Society of America, 108(2), 654-673, 2018.

LaHusen, S. R., Duvall, A. R., Booth, A. M., Grant, A., Mishkin, B. A., Montgomery, D. R., ... & Wartman, J.: Rainfall triggers more deep-seated landslides than Cascadia earthquakes in the Oregon Coast Range, USA. Science advances, 6(38), eaba6790, 2020.

Long, C. J., Whitlock, C., Bartlein, P. J., & Millspaugh, S. H.: A 9000-year fire history from the Oregon Coast Range, based on a high-resolution charcoal study. Canadian Journal of Forest Research, 28(5), 774–787. https://doi.org/10.1139/x98-051, 1998.

Milker, Y., Nelson, A. R., Horton, B. P., Engelhart, S. E., Bradley, L. A., & Witter, R. C.: Differences in coastal subsidence in southern Oregon (USA) during at least six prehistoric megathrust earthquakes. Quaternary Science Reviews, 142, 143–163. https://doi.org/10.1016/j.quascirev.2016.04.017, 2016.

Millspaugh, S. H., & Whitlock, C.: A 750-year fire history based on lake sediment records in central Yellowstone National Park, Holocene, 5, 283–292. https://doi.org/10.1177/095968369500500303, 1995.

Morey, A. E., Goldfinger, C., Briles, C. E., Gavin, D. G., Colombaroli, D., & Kusler, J. E.: Are great Cascadia earthquakes recorded in the sedimentary records from small forearc lakes? Natural Hazards and Earth System Sciences, 13, 2441–2463. https://doi.org/10.5194/nhess-13-2441-2013, 2013.

Mulder, T., Migeon, S., Savoye, B., & Faugères, J.-C.: Inversely graded turbidite sequences in the deep Mediterranean: A record of deposits from flood-generated turbidity currents? Geo-Marine Letters, 21(2), 86–93. https://doi.org/10.1007/s003670100071, 2001.

Nelson, A. R., Sawai, Y., Jennings, A. E., Bradley, L. A., Gerson, L., Sherrod, B. L., ... & Horton, B. P.: Great-earthquake paleogeodesy and tsunamis of the past 2000 years at Alsea Bay, central Oregon coast, USA. Quaternary Science Reviews, 27(7-8), 747-768, 2008.

Nelson, A. R., Kelsey, H. M., & Witter, R. C.: Great earthquakes of variable magnitude at the Cascadia subduction zone. Quaternary Research, 65(3), 354–365. https://doi.org/10.1016/j.yqres.2006.02.009, 2006.

Nelson, A. R., Hawkes, A. D., Sawai, Y., Horton, B. P., Witter, R. C., Bradley, L. A., & Cahill, N.: Minimal stratigraphic evidence for coseismic coastal subsidence during 2000 yr of megathrust earthquakes at the central Cascadia subduction zone. Geosphere, 2020.

Patton, J. R., Goldfinger, C., Morey, A. E., Ikehara, K., Romsos, C., Stoner, J., Djadjadihardja, Y., Ardhyastuti, S., Gaffar, E. Z., & Vizcaino, A.: A 6600 year earthquake history in the region of the 2004 Sumatra-Andaman subduction zone earthquake. Geosphere, 11(6), 2067–2129. https://doi.org/10.1130/GES01066.1, 2015.

Petersen, M. D., Shumway, A. M., Powers, P. M., Mueller, C. S., Moschetti, M. P., Frankel, A. D., ... & Zeng, Y.: The 2018 update of the US National Seismic Hazard Model: Overview of model and implications. Earthquake spectra, 36(1), 5-41, 2020.

Priest, G. R., Goldfinger, C., Wang, K., Witter, R. C., Zhang, Y., & Baptista, A. M.: Tsunami hazard assessment of the Northern Oregon coast: a multi-deterministic approach tested at Cannon Beach, Clatsop County, Oregon. Oregon Department of Geology Mineral Industries Special Paper, 41, 87, 2009.

Priest, G. R., Witter, R. C., Zhang, Y. J., Goldfinger, C., Wang, K., & Allan, J. C.: New constraints on coseismic slip during southern Cascadia subduction zone earthquakes over the past 4600 years implied by tsunami deposits and marine turbidites. Natural Hazards, 88(1), 285-313, 2017.

St-Onge, G., Mulder, T., Piper, D. J. W., Hillaire-Marcel, C., & Stoner, J. S.: Earthquake and flood-induced turbidites in the Saguenay Fjord (Québec): A Holocene paleoseismicity record. Quaternary Science Reviews, 23, 283–294. https://doi.org/10.1016/j.quascirev.2003.03.001, 2004.

Struble, W. T., Roering, J. J., Black, B. A., Burns, W. J., Calhoun, N., & Wetherell, L.: Dendrochronological dating of landslides in western Oregon: Searching for signals of the Cascadia AD 1700 earthquake. Geological Society of America, 2020.

Waldmann, N., Anselmetti, F. S., Ariztegui, D., Austin Jr, J. A., Pirouz, M., Moy, C. M., & Dunbar, R.: Holocene mass-wasting events in Lago Fagnano, Tierra del Fuego (54° S): implications for paleoseismicity of the Magallanes-Fagnano transform fault. Basin Research, 23(2), 171-190, 2011.

Wall, S. A., Roering, J. J., & Rengers, F. K.: Runoff-initiated post-fire debris flow Western Cascades, Oregon. Landslides, 1-13, 2020.

Walton, M.A., Staisch, L.M., Dura, T., Pearl, J.K., Sherrod, B., Gomberg, J., Engelhart, S., Tréhu, A., Watt, J., Perkins, J. and Witter, R.C.: Toward an integrative geological and geophysical view of Cascadia subduction zone earthquakes. Annual Review of Earth and Planetary Sciences, 49, pp.367-398, 2021.

Wang, P. L., Engelhart, S. E., Wang, K., Hawkes, A. D., Horton, B. P., Nelson, A. R., & Witter, R. C.: Heterogeneous rupture in the great Cascadia earthquake of 1700 inferred from coastal subsidence estimates. Journal of Geophysical Research: Solid Earth, 118(5), 2460–2473. https://doi.org/10.1002/jgrb.50101, 2013.

Witter, R. C., Kelsey, H. M., & Hemphill-Haley, E.: Great Cascadia earthquakes and tsunamis of the past 6700 years, Coquille River estuary, southern coastal Oregon. Geological Society of America Bulletin, 115(10), 1289-1306, 2003.

Witter, R. C., Zhang, Y., Wang, K., Goldfinger, C., Priest, G. R., & Allan, J. C.: Coseismic slip on the southern Cascadia megathrust implied by tsunami deposits in an Oregon lake and earthquake-triggered marine turbidites. Journal of Geophysical Research: Solid Earth, 117(B10), 2012.

Wright, H. E., Jr.: A square-rod piston sampler for lake sediments. Journal of Sedimentary Research, 37(3), 975. https://doi.org/10.1306/74D71807-2B21-11D7-8648000102C1865D, 1967.

Tables

Table 1. ***Sediment Cores. USL = Upper Squaw Lake; SQB = Lower Squaw Lake. Sediment core locations, water depth, and sediment-core lengths are listed for all cores used in this study. Cores highlighted in bold text are the primary core sites. Cores SQB6 and SQB7 are missing the historic portion of the record.***

Core name	Type	Length (m)	Water depth (m)	Latitude (°)	Longitude (°)
SQB-ss	Surface core	0.80	16.9	42.04405	-123.01853
SQB1	**Livingstone**	**6.74**	**16.9**	**42.04405**	**-123.01853**
SQB2	**Livingstone**	**7.37**	**16.5**	**42.04405**	**-123.01853**
SQB5	**Livingstone**	**3.98**	**23.5**	**42.04264**	**-123.01909**
SQB8	Kullenberg/Gravity	8.01	30.0	42.04227	-123.01908
SQB9	Kullenberg/Gravity	8.29	37.0	42.03982	-123.02050
SQB10	Kullenberg/Gravity	10.08	35.0	42.03857	-123.02108
SQB11	Kullenberg/Gravity	7.55	29.2	42.03778	-123.02175
SQB12	Kullenberg/Gravity	5.24	~20.0	42.04191	-123.01864
SQB13	Kullenberg/Gravity	6.24	25.0	42.02056	-123.02056
SQB14	**Kullenberg/Gravity**	**8.28**	**30.0**	**42.04356**	**-123.01836**
SQB15	Kullenberg/Gravity	4.55	28.5	42.04197	-123.01945
USL	**Livingstone**	10.2	14.1	42.19167	-123.09333

Table 2. Radiocarbon ages in radiocarbon years, and the ^{137}Cs peak (for Upper Squaw Lake core only; Colombaroli et al., 2010; 2018). The samples in gray text (Samples 0, and 11-13) were not included in the age model because they are inferred to be reworked. Samples in bold text were used to create the age-depth model for the historic portion of the sequence. Upper Squaw Lake depths are composite depths from splicing together two cores (Upper Squaw Lake I and Upper Squaw Lake II; collected in 2009) with overlapping 1-m drives to produce a continuous sequence; Colombaroli and Gavin, 2010. NOSAMS = National Ocean Sciences Accelerator Mass Spectrometry, SQB = Lower Squaw Lake, USL = Upper Squaw Lake. Sample ID's include the original sections and depths (archival and event-free composite) for the SQB cores, and composite depth for the USL cores.

Sample #	ID	Description	Laboratory and sample no.	^{14}C yrs BP
0	SQB1A; 14.0-14.5 cm	Fir needle	S-ANU 42418	865+/-35
1	**SQB1A; 15.5-16.0 cm event-free: 65 cm**	**Fir cone frag**	**S-ANU 42419**	**255+/-25**
2	**SQB1A; 25.5-26.0 cm Event-free: 71 cm**	**Fir needle**	**S-ANU 42618**	**110+/-25**
3	**SQB1A; 35.5-36.0 cm Event-free: 81 cm**	**Fir needle**	**S-ANU 42617**	**190+/-25**
4	**SQB1A; 84.0-85.0 cm Event-free: 108 cm**	**Fir needle**	**S-ANU 42616**	**260+/-40**
5	**SQB1A; 95.0-96.0 cm Event-free: 115 cm**	**decid. Plant frags**	**S-ANU 42417**	**630+/-25**
6	**SQB1B; 67.0-68.0 cm Event-free: 185 cm**	**plant frags**	**UCIAMS 140214**	**1155+/-20**
7	**SQB2H; 39.0 cm Event-free: 566 cm**	**plant frags**	**OS-109825**	**2480+/-20**
8	SQB5C; 27-28 cm	Cone bract	NOSAMS	1270+/-20
9	**SQB5D; 99-100 cm Event-free: 336 cm**	**Cone bract**	**NOSAMS**	**1580+/-20**
10	SQB14 sec 2, 81cm	Fir needle	NOSAMS	1220+/-20
11	SQB14 sec 3; 122.5cm	Twig	NOSAMS	2310+/-20
12	SQB14 sec 6; 30.5-31cm	Deciduous leaf	NOSAMS	4470+/-25
13	SQB10 sec 3, 54-55cm	Plant fragment	NOSAMS	1810+/-20
14	**USL; ^{137}Cs**	**Bulk samples**	**Flett Research, Inc.**	**~1964 CE**
15	USL; 539.5 cm	Charred wood	NOSAMS 64498	615+/-40
16	**USL; 630.5 cm Event-free: 145 cm**	**Terrestrial plant macros**	**NOSAMS 64497**	**980+/-55**
17	USL; 729 cm	Wood	Beta-23617	1110+/-40
18	USL; 856.5 cm	Bud scale	NOSAMS 64496	1610+/-140
19	USL; 952.5 cm	Douglas-fir needle	NOSAMS 64495	1870+/-100

Table 3. Calendar ages for deposits with characteristics of deposit J. Given are calibrated mean, mode and age ranges (95% confidence) in BP for the disturbance event deposits suspected to be Cascadia earthquakes in composite core SQBss/1/2. Those disturbance deposits in italics are less similar to deposit J as compared to the other deposits listed.

Event ID	depth (event-free; cm)	Cal yr BP Median	Cal yr BP Mean	2-sigma age range (Cal yr BP)
DE-H	58	100	100	60-130
DE-J	71	230	230	170-270
DE-K	101	370	360	280-460
DE-N	148	860	870	750-980
DE-O	207	1190	1200	1090-1280
DE-R	336	1490	1490	1430-1530
DE-S	*383*	*1710*	*1700*	*1520-1920*
DE-W	*496*	*2250*	*2250*	*2010-2500*
DE-X	522	2370	2380	2150-2600

Table 4. Comparison of Lower Squaw Lake chronology to those from Hydrate Ridge, Rogue and Bradley Lake records. Bold event ID's at left indicate those with characteristics similar to deposit J, whereas bold T#'s indicate thickest Rogue Apron beds. Blue ages are hemipelagic-derived ages whereas black indicates ages based on radiocarbon (but corrected to reflect the age of the deposit). For more information on marine ages see Goldfinger et al., 2012 (local ages, not averages, were used). The Bradley Lake data are the modified versions from Goldfinger et al., 2012. This was to use the youngest, rather than average, ages.

Event ID	Lower Squaw L.	Event	Bradley Lake	T#	Rogue Apron	Hydrate Ridge
DE-H	100 (60-130)					
DE-J	230 (170-270)	DE-1	250	**T1**	250 (200-300)	300 (230-410)
DE-K	370 (260-460)			T2	490 (380-590)	509 (410-610)
DE-L	590 (550-660)			T2a	550 (430-670)	
DE-M*	840 (740-960)					
DE-N	860 (750-980)	DE-2	940 (800-1060)	**T3**	740 (670-810)	800 (700-910)
		DE-3	1010 (930-1090)	T3a	1070 (970-1200)	1060 (950-1180)
DE-O	1200 (1080-1290)	DE-4	1360 (1300-1420)	**T4**	1200 (1100-1290)	1210 (1100-1340)
DE-P*	1370 (1260-1470)					
DE-Q	1390 (1290-1490)			T4a	1370 (1270-1500)	1470 (1330-1620)
DE-R	1490 (1410-1530)	DE-5	1520 (1370-1630)	**T5**	1560 (1400-1730)	1650 (1490-1813)
DE-S-1*	1700 (*1520-1930)*	DE-6	1540	T5a	1760 (1580-1930)	
DE-S-2*	undated					
DE-T	2020 (1760-2290)					
DE-U	2120 (1860-2390)			T5b	2020 (1850-2180)	
DE-V	2180 (1910-2430)					
DE-W	2250 (*2000-2500)*			T5c	2320 (2180-2470)	
DE-X	2380 (2140-2600)	DE-7	2550 (2350-2618)	T6	2560 (2490-2710)	2450 (2410-2720)
DE-Y	2510 (2340-2700)					
DE-Z	2580 (2370-2700)					
				T6a	2730 (2590-2880)	
				T6b	2820 (2680-2990)	
		DE-8	3120 (2960-3260)	**T7**	3060 (2860-3220)	2960 (2820-3070)

*Lower Squaw Lake DE's identified in gray (DE-M and DE-P) may be linked to DE's N and Q and not separate events. DE-S is separated into two (possibly three) individual events. The upper event is dated because it contains watershed-sourced sediment, whereas the lower ones do not. DE's in italics have inconclusive sedimentological characteristics as compared to deposit J.

Figures

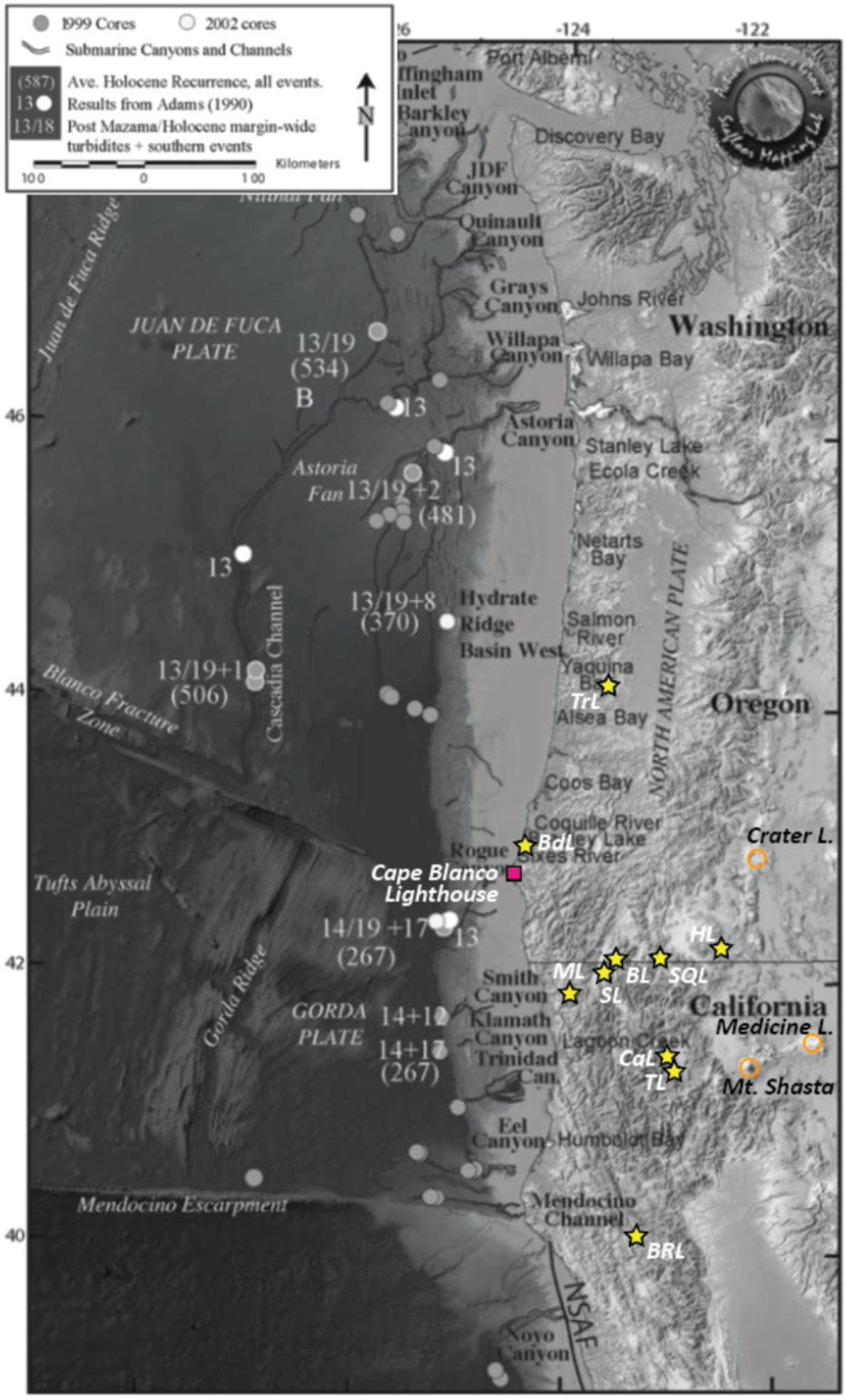

Figure 1

Location map. The yellow stars identify the location the lakes presented in this study (California: BRL = Black Rock Lake, TL = Taylor Lake, CaL = Campbell Lake, ML = Muslatt Lake, SL = Sanger Lake; Oregon: Bolan Lake, HL = Hobart Lake, BdL = Bradley Lake, TrL = Triangle Lake). Other sites mentioned in the text are at Sixes River, just south of BdL, and Coos Bay, just north of BDL. volcanoes are identified by orange circles. The base map (adapted from Goldfinger et al., 2012) identifies the location of channel systems and sediment cores used to reconstruct the offshore record of Cascadia earthquakes.

lower case d

missing L

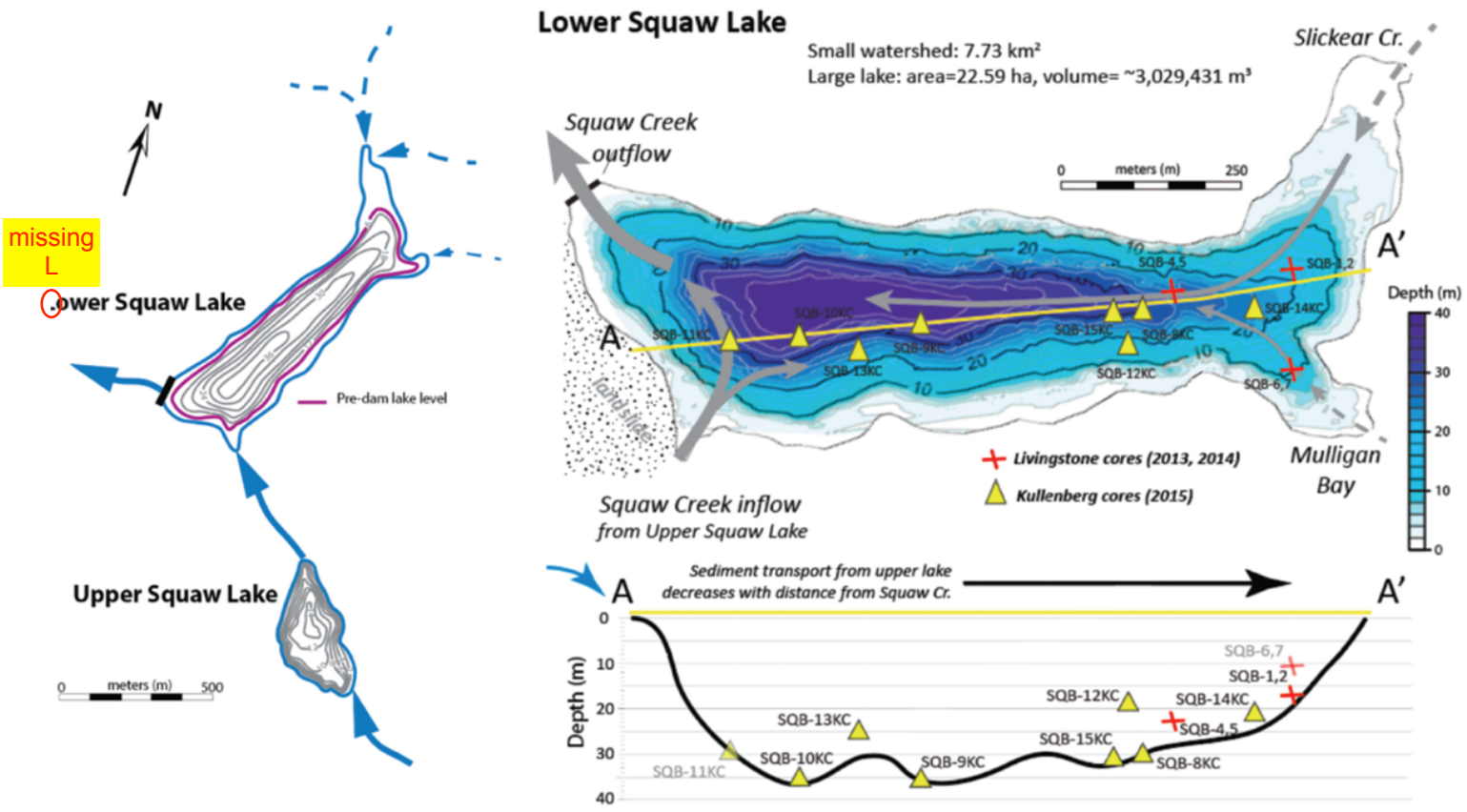

Figure 2

Lake Setting. Upper and Lower Lakes are shown with core locations. Left: The lakes are connected hydrologically by a small stream (Squaw Creek) that crosses a portion of the landslide that created Upper Squaw Lake. Right: The core locations for each of the sediment cores from Lower Squaw Lake are identified by triangles (2015 cores) or X's (2013 and 2014; red). The Upper Squaw Lake core was taken from 14.1 m water depth, at the lake's depocenter.

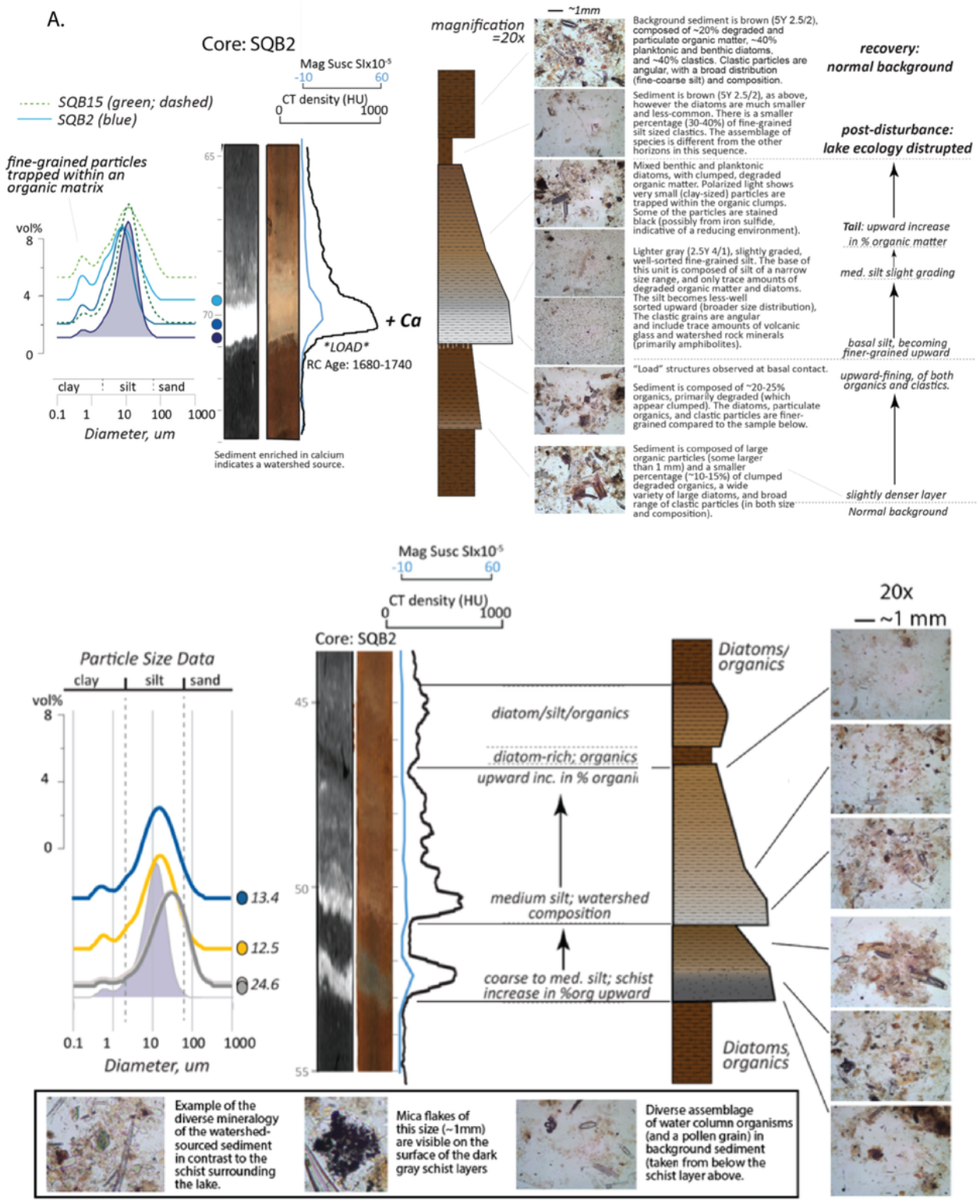

Figure 3

Characteristics of earthquake-triggered deposits, as described in Morey et al., submitted; this volume. A. Type 1 earthquake deposit, attributed to the 1700 CE Cascadia earthquake, has load structures below the deposit base, followed by a fine-grained, well-sorted silt layer sourced from the watershed (indicated by the presence of calcium minerals), followed by a long, organic-rich tail. B. Type 2 earthquake deposit is a

turbidite composed of lake-margin-sourced schist (represented by the lower schist deposit in this sequence; deposit I). This deposit was attributed to the 1873 CE earthquake deposit.

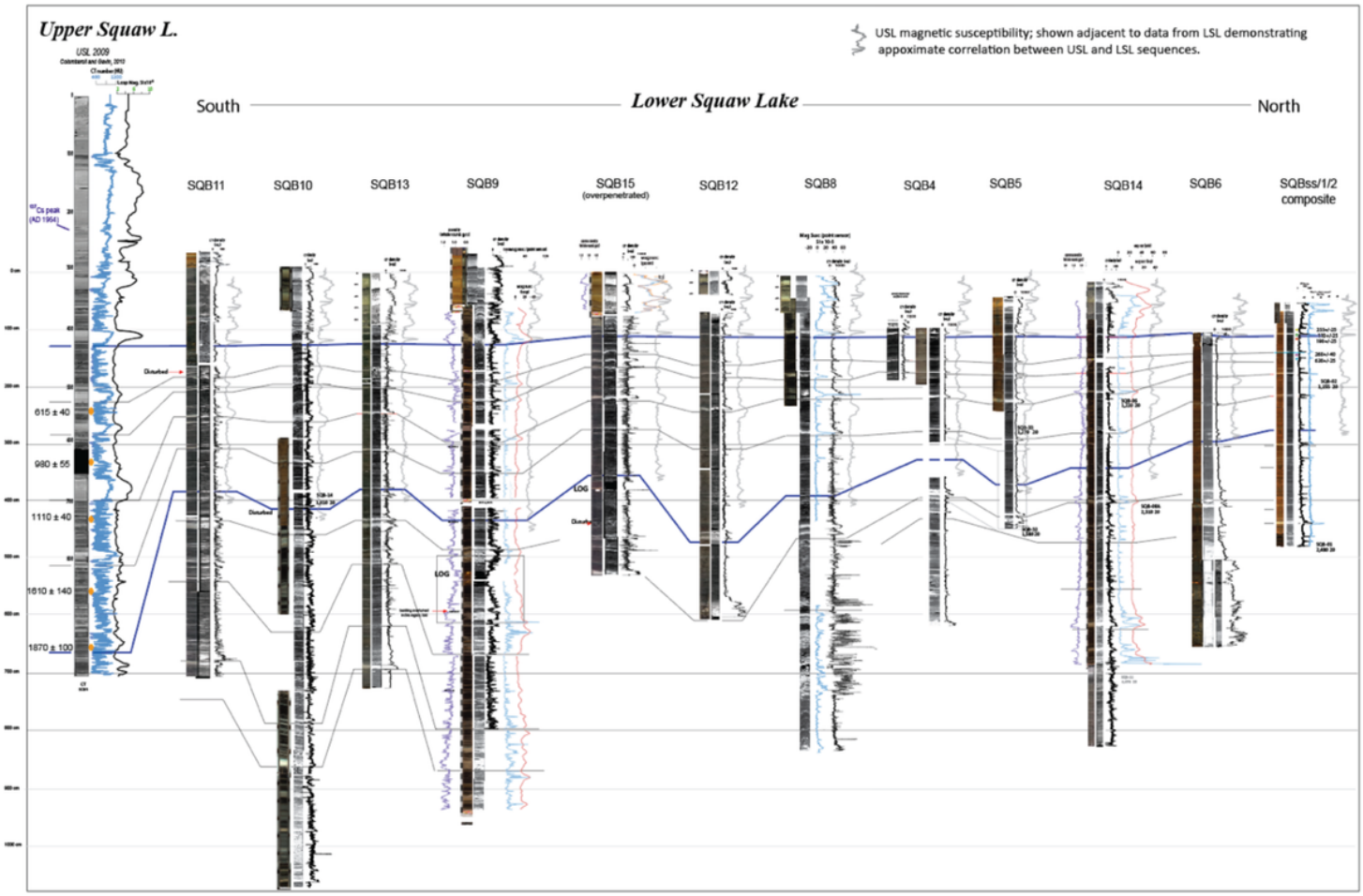

Figure 4

Correlation diagram for all cores in Lower Squaw Lake and relationship to the Upper Squaw Lake core. Cores are hung on the lake-wide disturbance deposit J, suggested in the companion manuscript (Morey et al., submitted, this volume) to be the result of the 1700 CE Cascadia earthquake. The thick line connects deposits that are the result of a disturbance from around ~1500 BP.

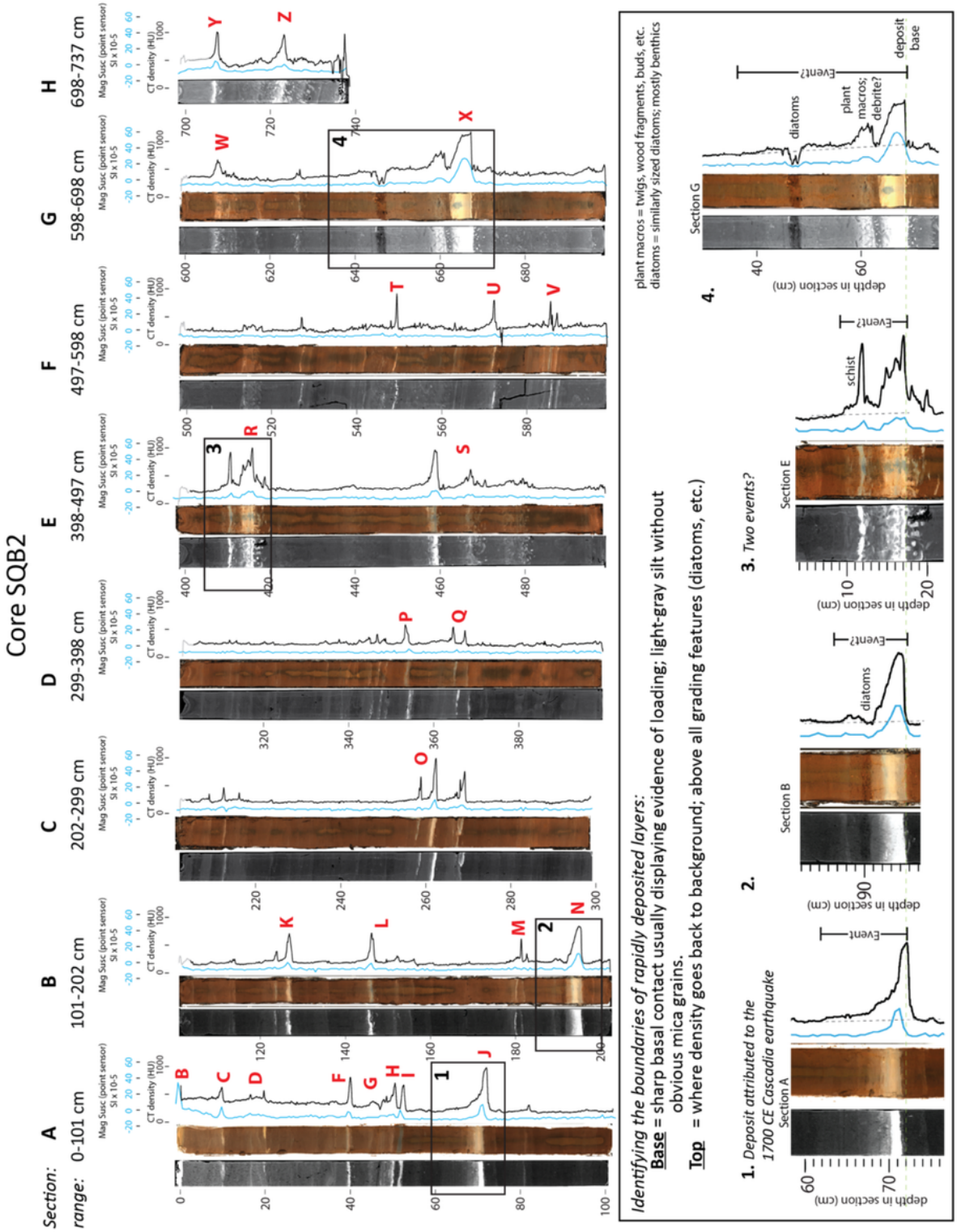

Figure 5

Changes in expression of earthquake deposits downcore in SQB2. Archival depths are in cm below the core top. Deposits identified by red letters are disturbance deposits that are evaluated in this manuscript. Those identified by numbered boxes are illustrate the complexity and variability in the expression of these disturbance deposits downcore.

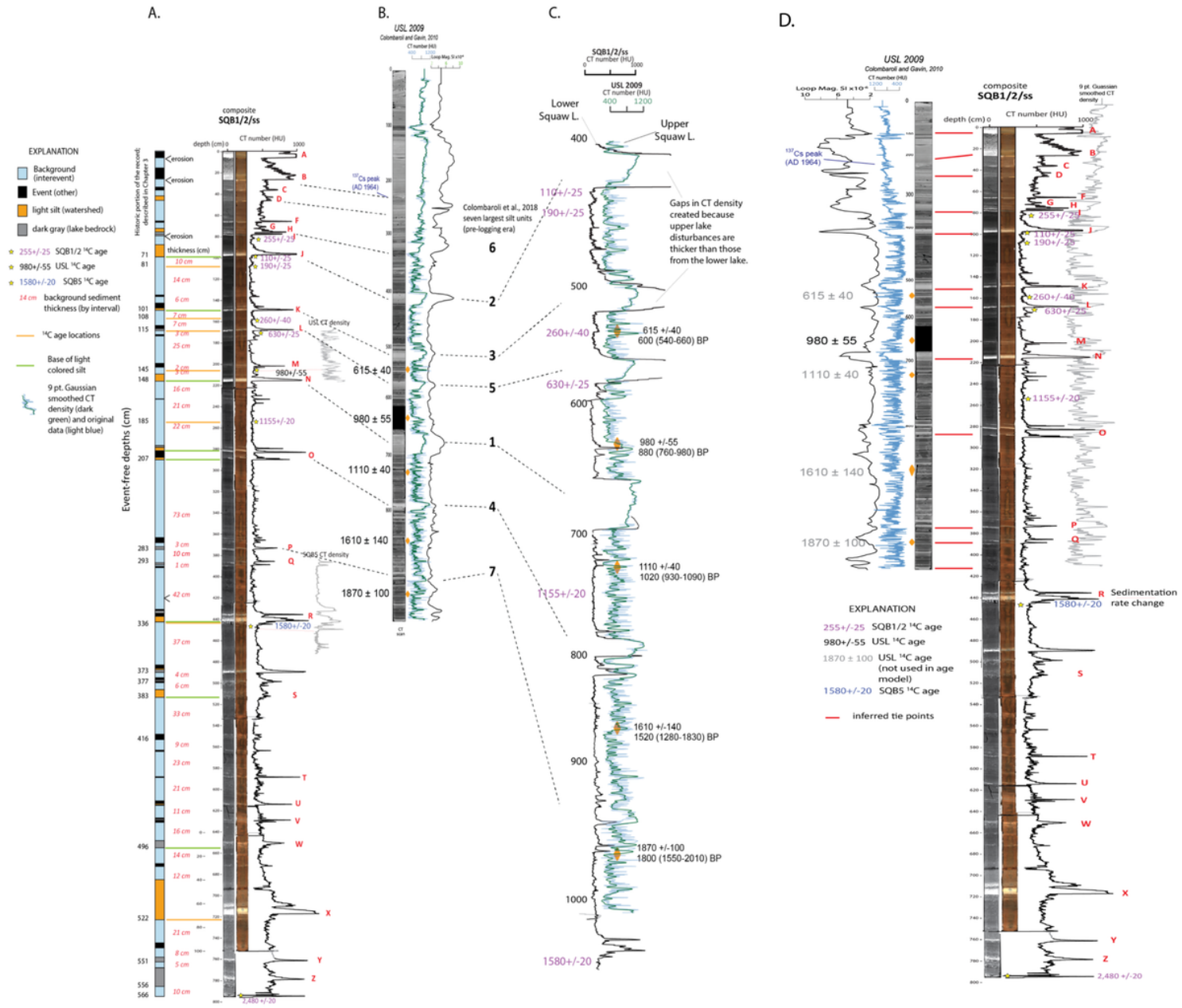

Figure 6

Identification of disturbance deposits and correlation between upper and lower lake records. A. Red numbers represent the interevent thicknesses used in the event-free age-depth model. The red capital letters A-Z indicate the disturbances identified in this study. Gray traces to the right identify correlative sequences where age data have been used to supplement those radiocarbon determinations in core SQB1/2/ss. B. The relationship to the 2009 Upper Squaw Lake core is shown by correlation lines (dashed). C. The relationship between the CT density data from core SQB1/2/ss (black trace) is shown compared to the CT density data from the upper lake core (green trace; 9 point Gaussian smoothing is shown over original data in blue). The relationships to the seven thickest deposits in the upper lake record compared to the lower lake record identified in Colombaroli et al., 2018 are identified by the dashed lines connecting numbers to events in the sequence. Note that the depth scale for the USL core (CT units shown in blue) are true, but the depth of the lower lake core (CT units shown in black) are not shown

because depths have been distorted to match events. This is called flattening. Breaks in the lower lake CT data were made in the middle of each thick deposit because the thicknesses of the upper lake deposits are much greater than the thicknesses of the lower lake deposits. Note that ages with +/- are radiocarbon determinations, and those with ranges in parentheses are calendar ages. See the Explanation for details.

d. *USL 2009 (left) was flattened to core SQB1/2/ss (right) to demonstrate the similarities between the core data*. Flattening is a method whereby all the core data are transformed to match correlative horizons, in this case, correlative deposit bases. Correlated bases are identified by the red tie lines between cores. The correlation suggests that the radiocarbon ages identified in gray are older than the radiocarbon data would suggest for the lower lake core. Note that whole round magnetic susceptibility is in black and CT density is in blue (for core USL 2009) and CT density is in black for the core SQB1/2/ss. The gray trace to the far right is the USL 2009 smoothed CT density (9 point Gaussian window) to better compare the records (because the data in the upper lake core contains many more silt layers than the lower lake core).

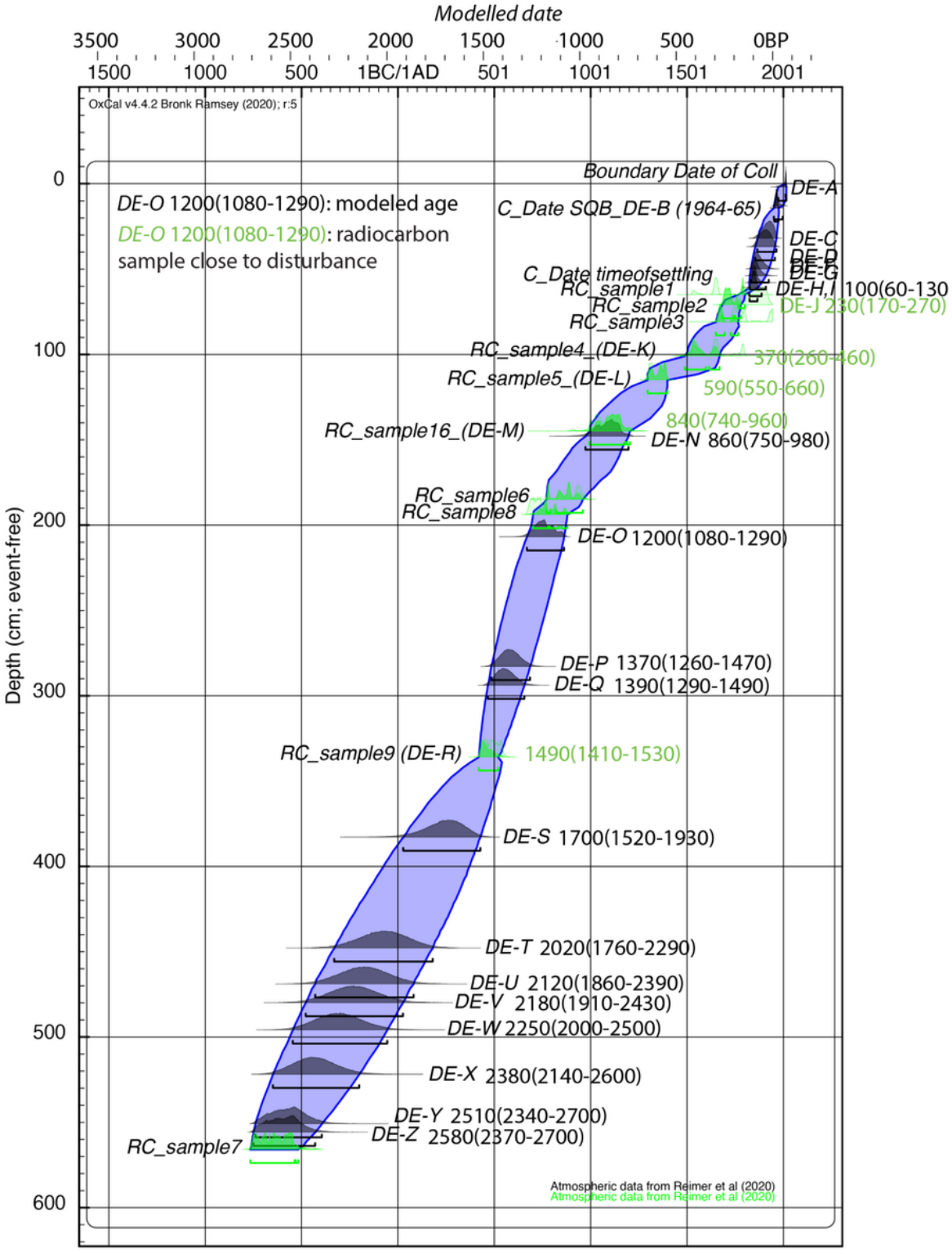

Figure 7

Downcore age-depth model for Lower Squaw Lake composite core SQBss/1/2. Sample numbers (refer back to Table 2) are positioned adjacent to their distributions. The envelope reflects the uncertainty (95% confidence) of the age-depth curve. Calendar ages in black are modeled ages and those in green are modeled ages by radiocarbon samples in close proximity to a disturbance deposit.

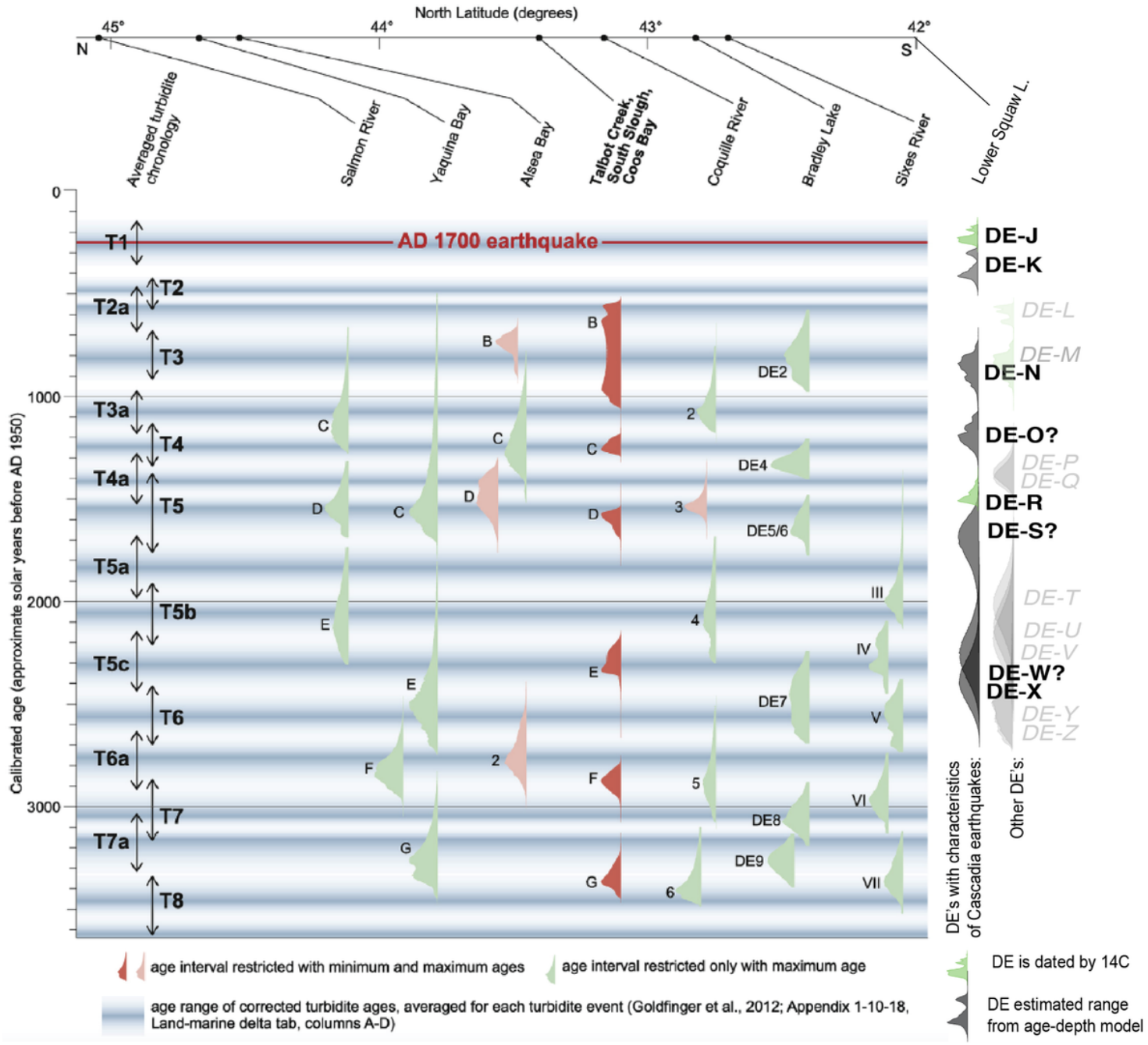

Figure 8

Comparison of the Lower Squaw Lake earthquake chronology to the compilation of southern Cascadia paleoseismic records by Milker et al., 2016. At the far left are the marine age ranges of corrected turbidite, margin-wide averages (corrected for reservoir age) from Goldfinger 2012. At the far right are the disturbance deposits distributions for deposits K, N, O, R, S, W and X which are most similar to deposit J. Those distributions in green are deposits that have been directly dated. The other distributions in lighter gray are the remaining disturbances in the sequence that have other characteristics (schist layers and thinner, less distinct, layers).

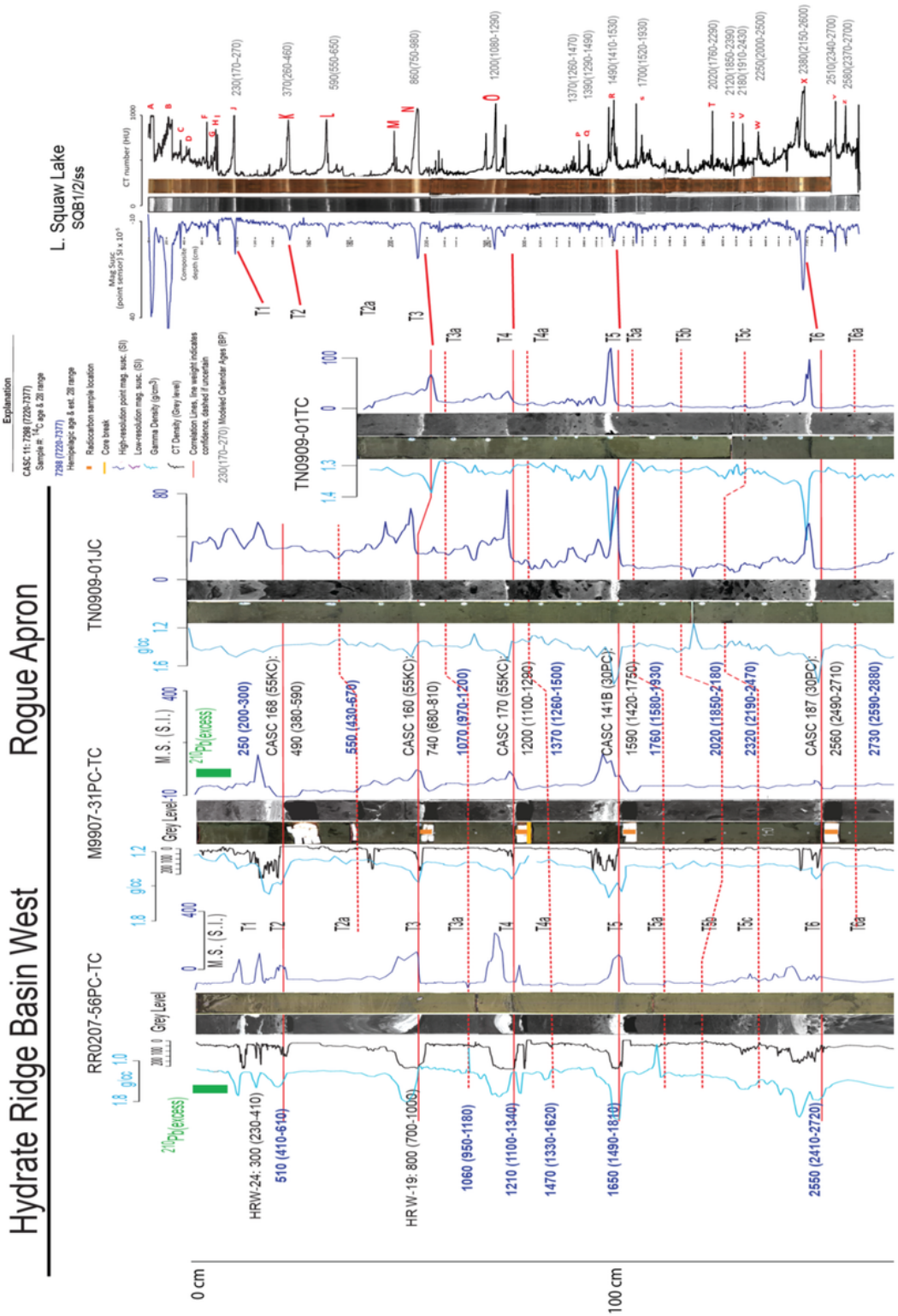

Figure 9

Correlation diagram. This diagram shows bed relationships for correlative units between Lower Squaw Lake, Rogue Apron and Hydrate Ridge Basin West paleoseismic sites.

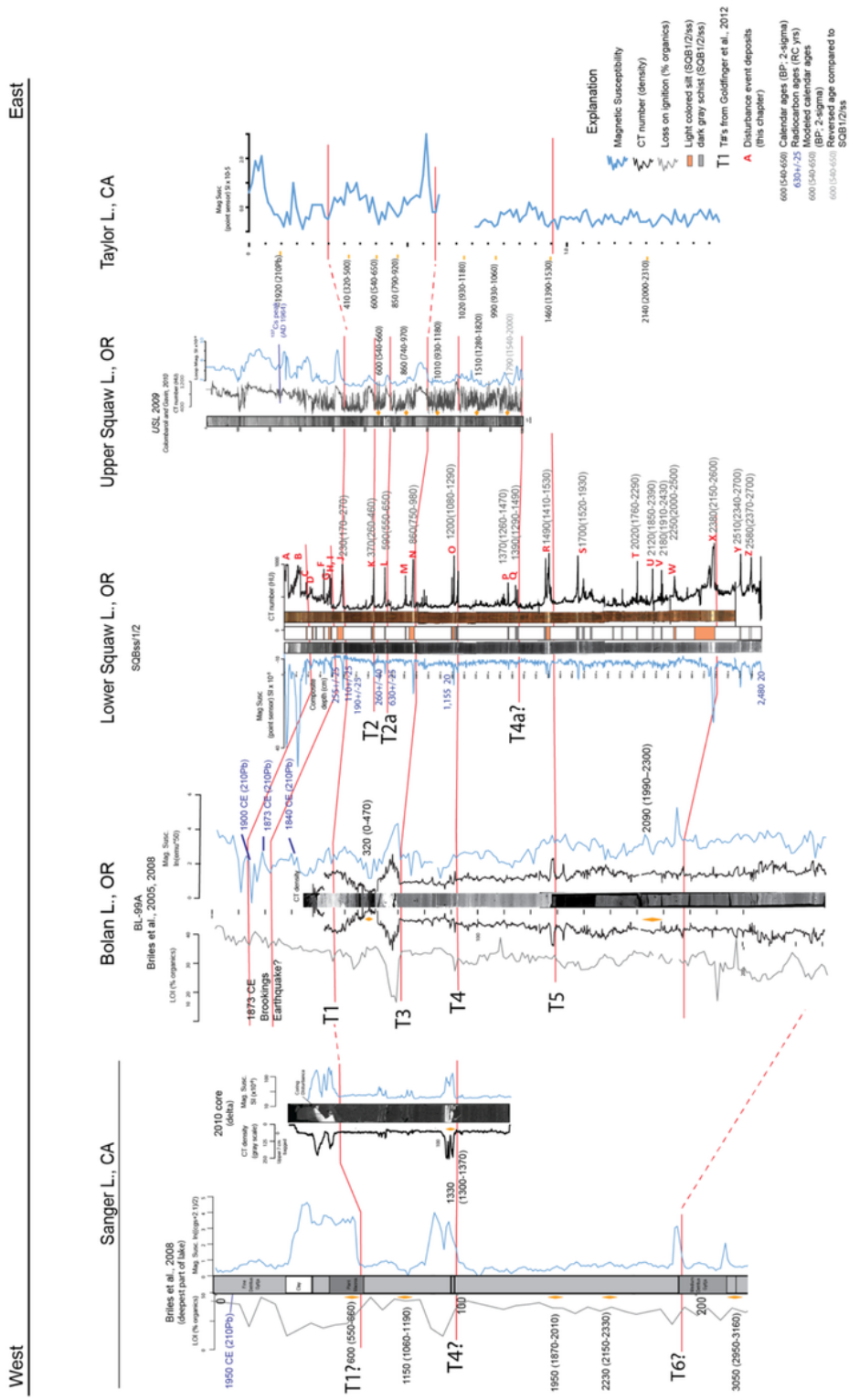

Figure 10

Correlated disturbance deposits in lake sediments near the California/Oregon border (Figure 1 map for the locations of the lakes). Disturbance event deposits are shown as increases in CT density, magnetic susceptibility and loss on ignition data). Physical property signatures and radiocarbon age data allow beds to be correlated regionally. T1-T3 identify inferred relationships with marine sediment core events

from Goldfinger et al., 2012. Solid red lines identify the most confident ties between cores, and less-certain where dashed.

Supplementary Files

This is a list of supplementary files associated with this preprint. Click to download.

- Supplementarydata.docx